Engineering Development Studies for Molten-Salt Breeder Reactor Processing No. 21

OAK RIDGE NATIONAL LABORATORY

ENGINEERING DEVELOPMENT STUDIES FOR MOLTEN-SALT
BREEDER REACTOR PROCESSING NO. 21

Compiled by:

J. R. Hightower, Jr.

Other Contributors:

C. H. Brown, Jr.
R. M. Counce
R. B. Lindauer
H. C. Savage
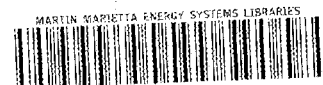
MARCH 1976

Reports previously issued in this series are as follows:

ORNL-TM-3053	Period ending December 1968
ORNL-TM-3137	Period ending March 1969
ORNL-TM-3138	Period ending June 1969
ORNL-TM-3139	Period ending September 1969
ORNL-TM-3140	Period ending December 1969
ORNL-TM-3141	Period ending March 1970
ORNL-TM-3257	Period ending June 1970
ORNL-TM-3258	Period ending September 1970
ORNL-TM-3259	Period ending December 1970
ORNL-TM-3352	Period ending March 1971
ORNL-TM-4698	Period January through June 1974
ORNL-TM-4863	Period July through September 1974
ORNL-TM-4870	Period October through December 1974

CONTENTS

SUMMARIES

CONTINUOUS FLUORINATOR DEVELOPMENT: AUTORESISTANCE HEATING TEST AHT-4

After completion of the third autoresistance heating test (AHT-3), the system was dismantled and the test vessel was decontaminated for use in the next test, AHT-4. Design and fabrication for the other vessels to be used in AHT-4 were completed and installation was begun.

DEVELOPMENT OF THE METAL TRANSFER PROCESS

Engineering experiments to study the steps in the metal transfer process for removing rare-earth fission products from a molten-salt breeder reactor fuel salt will be continued in experiment MTE-3B. During this report period, we completed preoperational testing of the facility; charging of the salt and bismuth phase to the process vessels is in progress.

SALT-METAL CONTACTOR DEVELOPMENT: EXPERIMENTS WITH A MECHANICALLY AGITATED, NONDISPERSING CONTACTOR IN THE SALT-BISMUTH FLOWTHROUGH FACILITY

The eighth and ninth tracer runs (TSMC-8 and -9) were completed in the mild steel contactor installed in the salt-bismuth flowthrough facility in Bldg. 3592. The agitator drive assembly failed to operate properly during run TSMC-8. The assembly was dismantled, repaired, and reassembled, with resultant satisfactory operation. Run TSMC-9 was made at a high agitator speed (244 rpm) to determine both the mass transfer coefficient under conditions in which salt is dispersed into the bismuth, and if large amounts of bismuth and salt are entrained in the other phase. The mass transfer coefficient was 0.121 ± 0.108 cm/sec, which is 178% of the Lewis correlation. All the data suggest that when the phases are not dispersed, the effect of agitator speed on the mass transfer coefficient is less than that predicted by the Lewis correlation.

SALT-METAL CONTACTOR DEVELOPMENT: EXPERIMENTS WITH A MECHANICALLY AGITATED, NONDISPERSING CONTACTOR USING WATER AND MERCURY

Mass transfer rates between water and mercury have been measured in a mechanically agitated contactor using the reaction:

$$Pb^{2+}(H_2O) + Zn(Hg) \rightarrow Zn^{2+}(H_2O) + Pb(Hg) \, ,$$
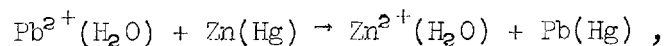
which was assumed to be instantaneous, irreversible, and occurring entirely at the water-mercury interface.

Several runs were made in the water-mercury contactor at an elevated temperature ($\sim 40°C$) to test the validity of the assumption that the interfacial reaction given above is instantaneous. Results from these runs were inconclusive.

Investigation was initiated to determine if polarography is a viable alternate method for measuring mass transfer rates in a stirred interface contactor using mercury and an aqueous electrolyte solution. Several electrolyte solutions were investigated, but none were found to be entirely inert to mercury. Information found in the literature suggested that a Fe^{2+}-Fe^{3+} redox couple (using iron complexed with oxalate ions) may be suitable as an electrolyte for our application. Further tests will be performed to determine if the iron electrolyte will produce suitable polarograms.

FUEL RECONSTITUTION DEVELOPMENT: INSTALLATION OF EQUIPMENT FOR A FUEL RECONSTITUTION ENGINEERING EXPERIMENT

Salt used in experiment AHT-3 was treated with H_2 and HF to remove oxides. This salt will be used in the first fuel reconstitution experiments. Installation of the fuel reconstitution experimental equipment is continuing.

1. INTRODUCTION

A molten-salt breeder reactor (MSBR) will be fueled with a molten fluoride mixture that will circulate through the blanket and core regions of the reactor and through the primary heat exchangers. We are developing processing methods for use in a close-coupled facility for removing fission products, corrosion products, and fissile materials from the molten fluoride mixture.

Several operations associated with MSBR processing are under study. The remaining parts of this report discuss:

  (1) decontamination of the test vessel used in autoresistance heating test AHT-3, and the design of equipment for autoresistance heating test AHT-4;

  (2) progress on installation of metal transfer experiment MTE-3B;

  (3) measurements of mass transfer of ^{237}U and ^{97}Zr from MSBR fuel carrier salt to molten bismuth in a mechanically agitated contactor;

  (4) results of an investigation to determine if polarography is a suitable method for measuring water-side mass transfer coefficients in a mechanically agitated contactor operating with water and mercury; and

  (5) description of equipment to be used in engineering studies of fuel reconstitution.

This work was performed in the Chemical Technology Division during the period January through March 1975.

2. CONTINUOUS FLUORINATOR DEVELOPMENT: AUTORESISTANCE HEATING TEST AHT-4

R. B. Lindauer

After completion of the third autoresistance heating test (AHT-3), the system was dismantled and the test vessel was decontaminated for use in the next test, AHT-4. Design and fabrication for the other vessels to be used in AHT-4 were completed and installation was begun.

2.1 Decontamination of AHT-3 Test Vessel

The test vessel was cleaned by treating it with hot (∿ 200°F) 6% oxalic acid in an open steam-heated vat. In order to submerge the vessel completely in the 14- to 20-in. depth of solution, it was first necessary to cut the vessel below the electrode side arm, since this side arm and the gas-inlet side arm are not in the same plane. The bottom of the vessel, which contained a 2-in. salt heel, was removed before immersion. After 3 days, the solution was drained and the vessel was inspected. Salt remained below the gas-inlet side arm, and the electrode was still secured in the side arm by some residual salt. Evidently the salt had contained sufficient crud to prevent complete drainage through the side-arm drain line. A sample of the material taken from below the gas inlet contained 58% thorium.

The vessel was treated for an additional 3 days in a second oxalic acid bath. It was then possible to remove the electrode and chip out the remaining salt in the side arm. A survey of the vessel revealed considerable transferable activity. The vat was cleaned and the vessel was treated with a solution of ammonium oxalate and Versene. After this treatment, the metal surface had a shiny metallic appearance, compared with the dull, powdery look on the surface after the oxalic acid treatments. A third oxalate treatment was made followed by wet sand blasting. A final survey showed < 200 dpm of transferable activity.

2.2 Design of Equipment for Autoresistance Heating Test AHT-4

The next test of autoresistance heating for the frozen wall fluorinator will use a circulating salt system to help prevent complete freezing in the test vessel. The flowsheet for this test is shown in Fig. 1. Salt flows from the surge tank to the gas-liquid separator by means of an argon gas lift. The salt then flows by gravity to the test vessel where it enters through a special insulated flange and the electrode. The salt leaves the bottom of the test vessel and passes through a heat flowmeter before being returned to the surge tank through another insulated flange. The insulated flanges are water-cooled to permit the use of Teflon gaskets. The bolts are insulated by a Bakelite sleeve and Teflon washers, as shown

OFF-GAS

GAS-LIQUID
SEPARATOR

ARGON FOR
GAS LIFT

FREEZE
VALVE

AUTORESISTANCE
HEATING POWER
SUPPLY

ARGON

HEAT
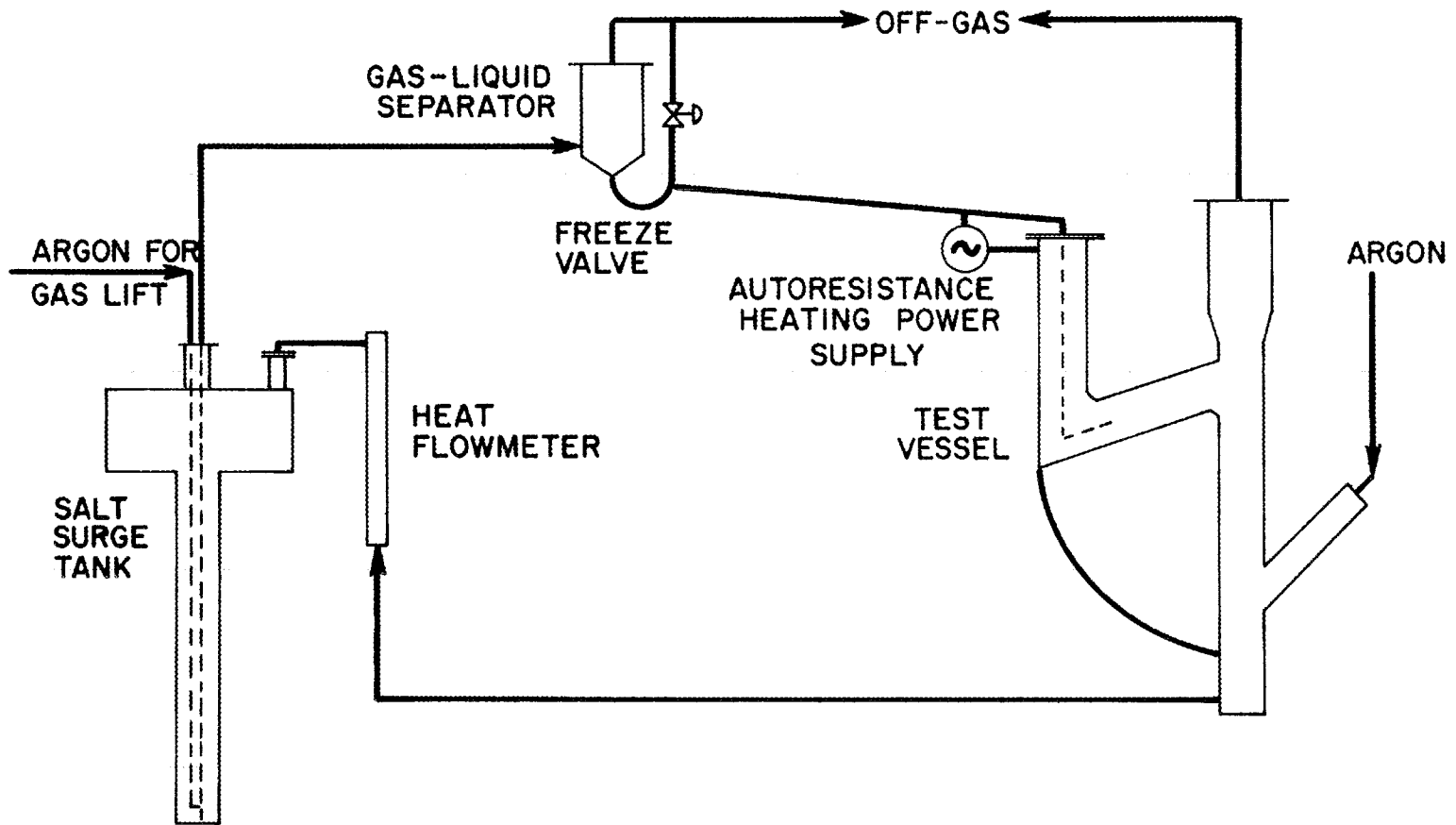FLOWMETER

TEST
VESSEL

SALT
SURGE
TANK

Fig. 1. Flowsheet for autoresistance heating test AHT-4.

in Fig. 2. The return line has a deflector at the point at which it enters
the surge tank to prevent short-circuiting across the liquid stream (Fig. 3).
The surge tank and separator are, therefore, at the same electrical poten-
tial as the electrode and must be insulated from the equipment supports.
Gas lines to these two vessels have insulated sections. An air-cooled
freeze valve is located in the line between the separator and the test
vessel to make it possible to transfer the molten salt from the test
vessel to the surge tank after a run to determine the film thickness.

The individual equipment pieces are described below.

Test vessel. The test vessel is the same one used in AHT-3. After
draining salt from the last run, inspection of the vessel revealed about
11 liters of material which failed to drain. This was due partly to
runback, but was primarily caused by plugging of the side-arm drain line
with impurities (oxides and structural metal fluorides) which had
accumulated over the past 2 years. The bottom 6-1/2 in. of the vessel
was filled with salt and was cut off. Another cut was made below the
electrode side arm to allow submergence in an open vat. The test vessel
was treated with a hot (~ 200°F) 6% oxalic acid solution for 7 days, and
hot ammonium oxalate for 2 days. The solution was changed twice during
the cleaning. Cleaning was complicated by the salt remaining in the
electrode side arm which prevented removal of the electrode and flange.
This also prevented circulation of the oxalic acid through the side arm.
After the electrode was broken loose, the residual salt was broken up
manually and decontamination was completed. New heaters and cooling coils
have now been installed on the test vessel for better control of tempera-
ture. The electrode, Fig. 4, is similar to that used in AHT-3, but with
an open-end pipe for salt flow.

Fluoride-salt surge tank (Figs. 5 and 6). This is a dual diameter
vessel with a lower section of 6-in. sched 40 nickel pipe, 46-in. long;
the upper section is 1/8-in-thick nickel, 24 in. in diameter by 11-in.
high. The long 6-in. section provides ample submergence for the gas
lift, while the large diameter upper section provides sufficient capacity
to contain the salt from the entire system. A sensitive (0.20 in. of
water) liquid-level instrument in the large diameter section will indicate
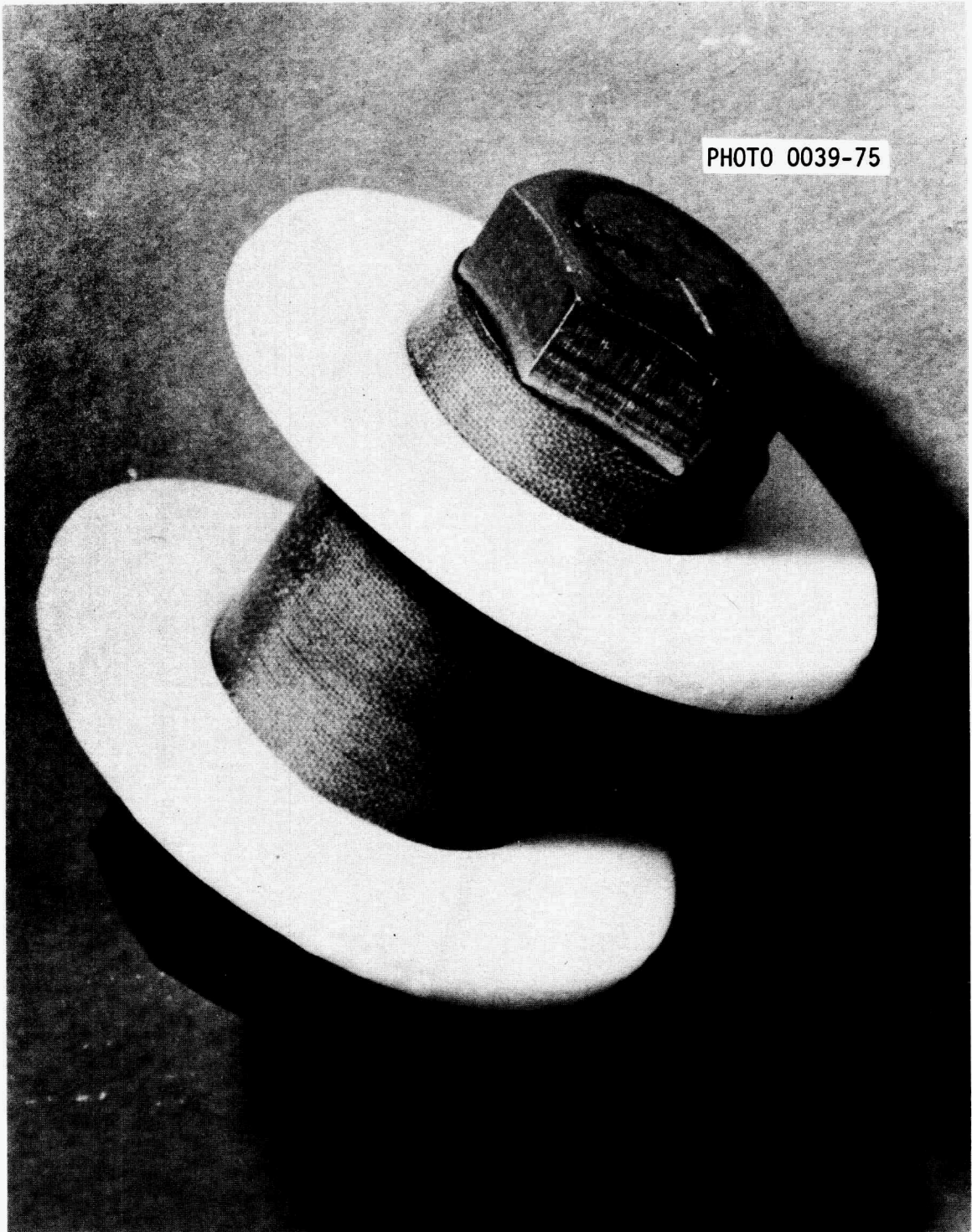
PHOTO 0039-75

Fig. 2.   Insulated bolts used with electrical isolation flanges.

PHOTO 0042-75
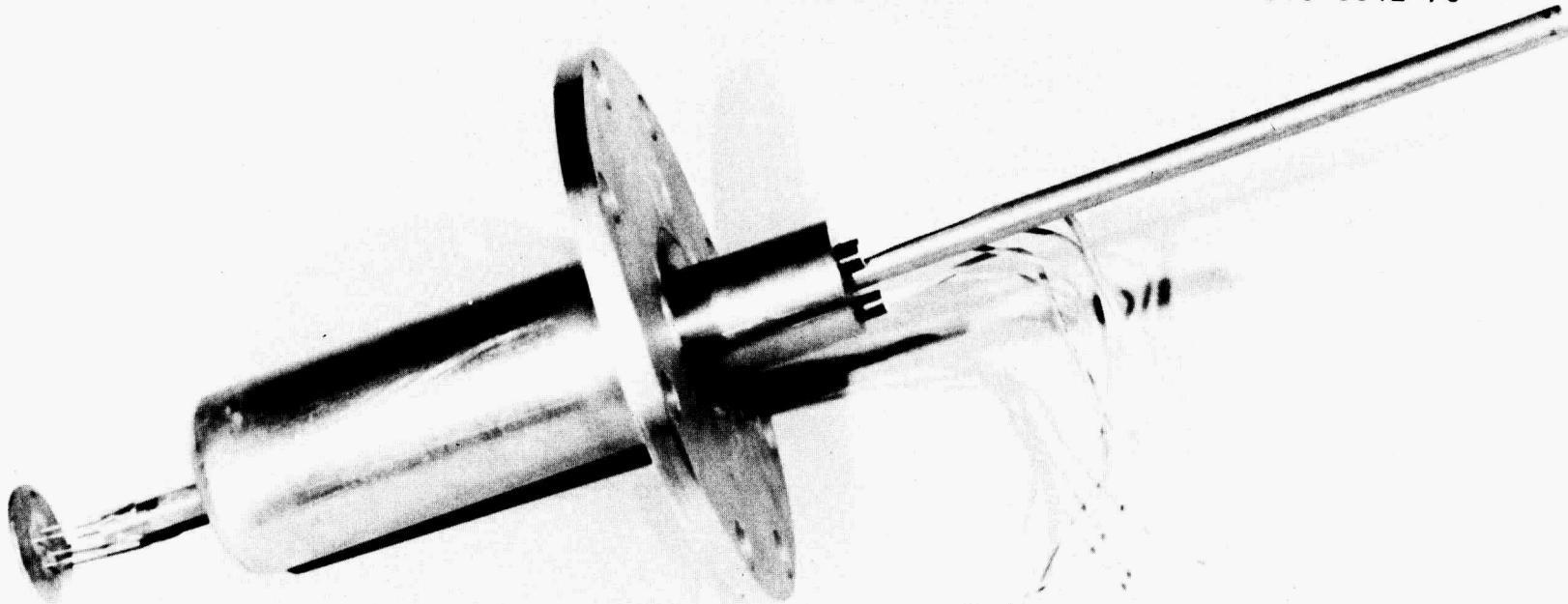
Fig. 3. Electrical isolation flange for salt return line to surge tank.
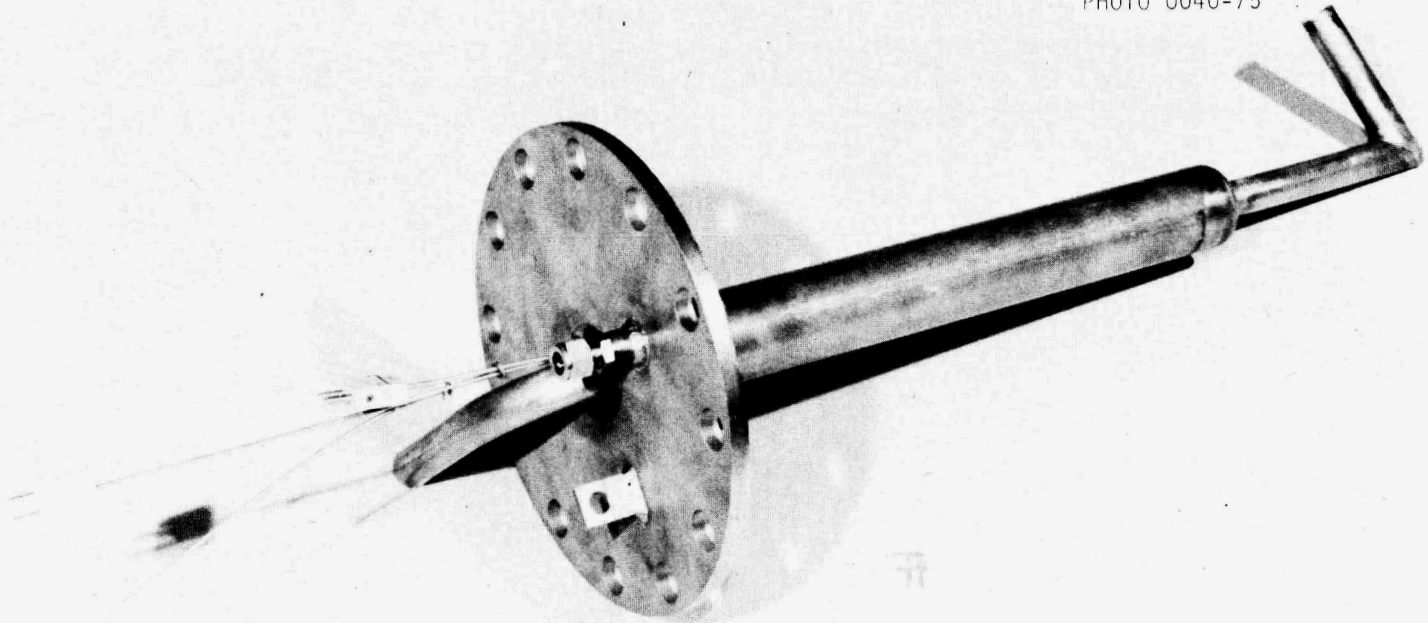
Fig. 4. Electrode to be used in test vessel of autoresistance
heating test AHT-4.

PHOTO 0038-75
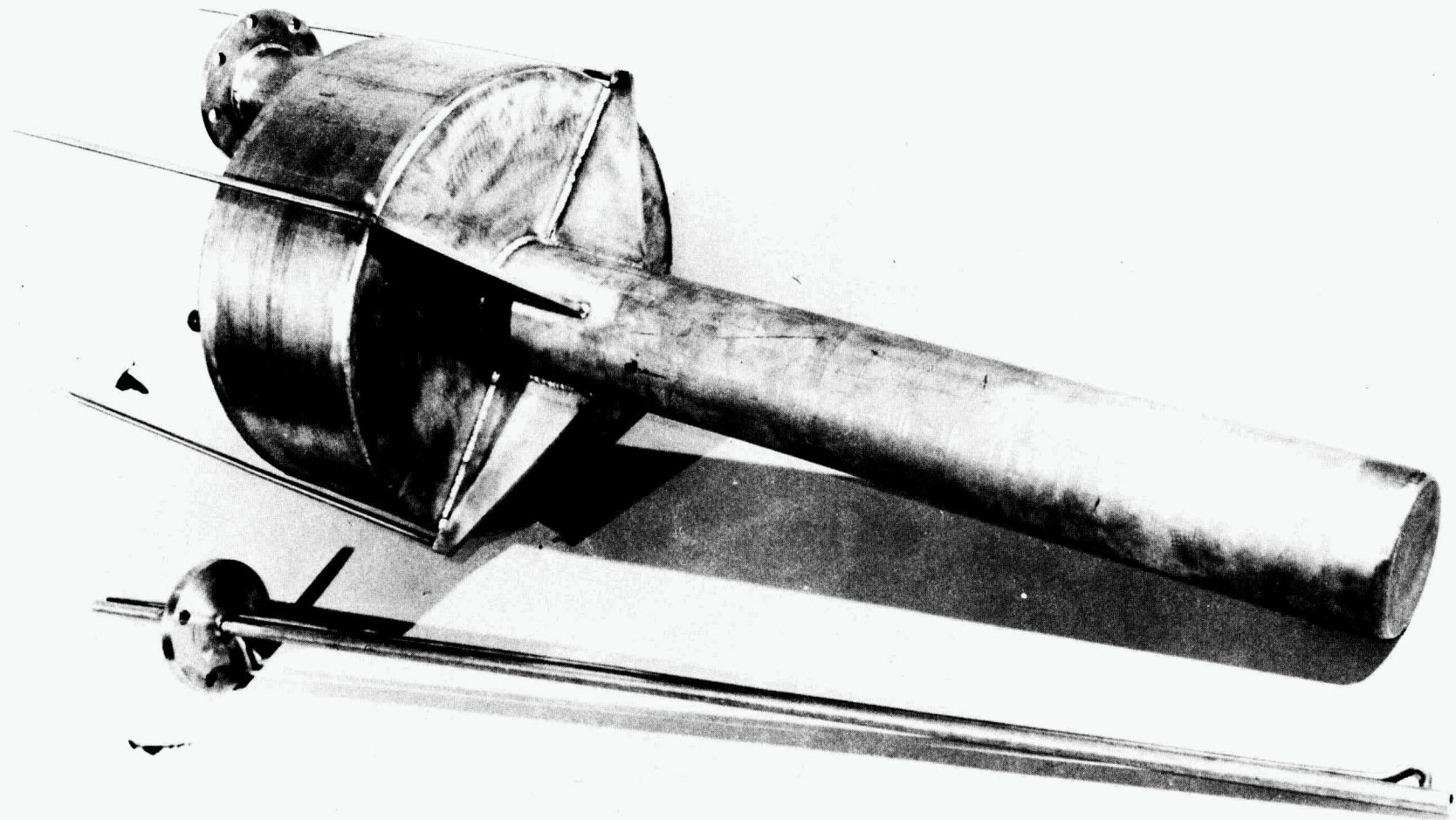
Fig. 5. Top view of surge tank.
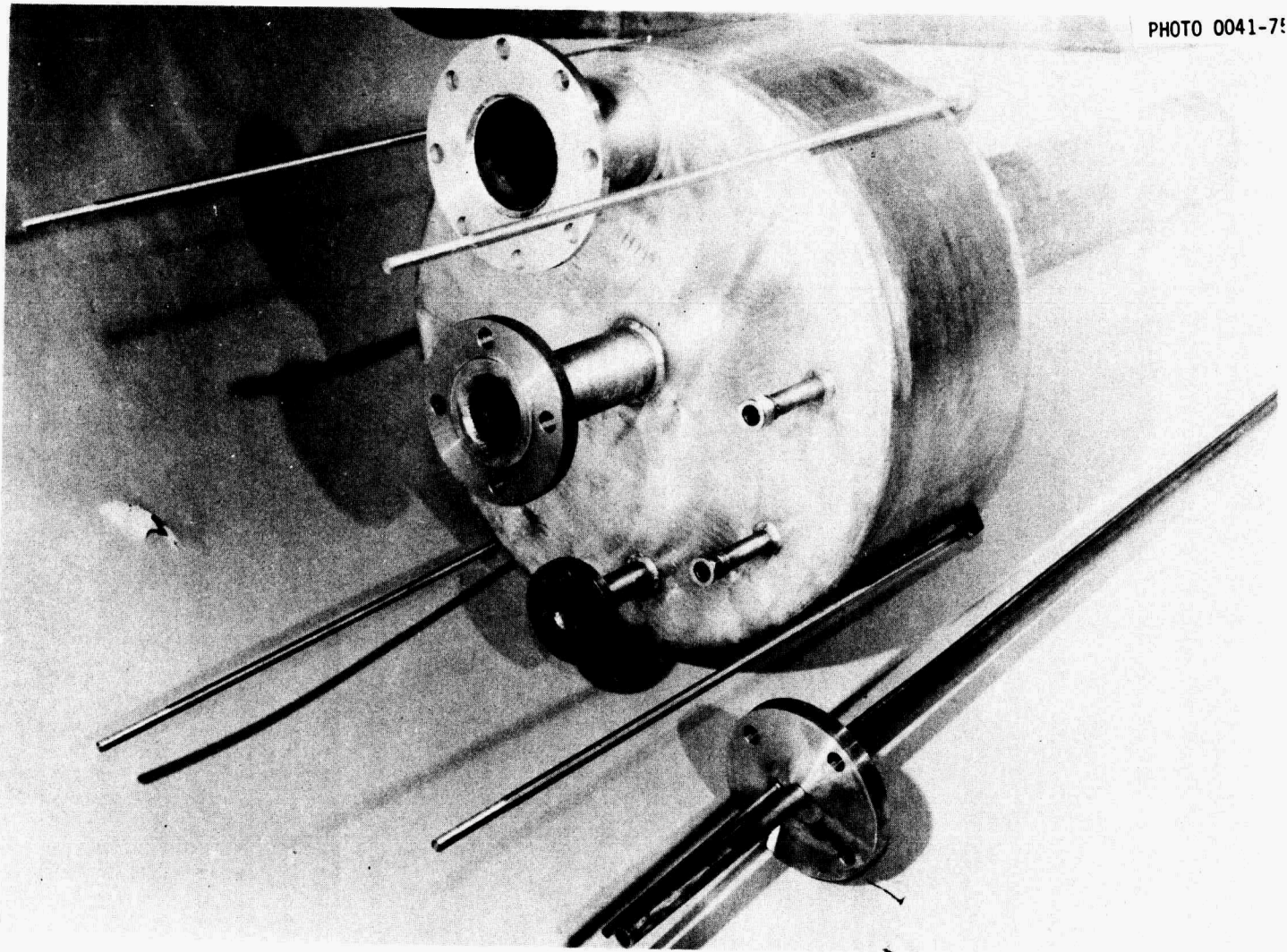
Fig. 6. Bottom view of surge tank.

PHOTO 0041-7!

any unusual buildup of salt at the top of the test vessel or separator, as well as providing a means for measuring the volume of the frozen salt film after a test run.

Gas-liquid separator. This is an 8-in.-diam by 12-in.-high cone-bottom nickel vessel containing an 8-in.-deep demister of nickel York-mesh. Two baffle plates are located below the Yorkmesh for separation of the bulk of the argon and salt from the gas lift. A differential pressure instrument will detect any liquid buildup in the bottom or any excessive pressure drop across the separator. A thermowell is located in the Yorkmesh which will be maintained above the melting point of the salt.

Heat flowmeter. The salt leaving the test vessel passes through a 28-in. section of 2-in. nickel pipe containing a cartridge heater. Heat loss from the flowmeter (Fig. 7) will be balanced by external heaters. The internal heater can be operated on either 120 V (750 W) or 240 V (3000 W), depending on the salt flow rate. A temperature rise of about 10°C through the flowmeter will indicate a salt flow rate of either 0.9 or 3.6 liters/min, depending on whether the voltage applied to the cartridge heater is 120 V or 240 V.

3. DEVELOPMENT OF THE METAL TRANSFER PROCESS
H. C. Savage

Engineering experiments to study the steps in the metal transfer process for removing rare-earth fission products from a molten-salt breeder reactor fuel salt will be continued in experiment MTE-3B.[1] During this report period, we completed preoperational testing of the facility, and the charging of the salt and bismuth phases to the process vessels is in progress.

3.1 Status of Metal Transfer Experiment MTE-3B

After installation, the three process vessels (fluoride fuel salt reservoirs, contactor, and stripper) were heated to the design operating temperatures of 650°C under an inert gas (argon) atmosphere, and were pressure tested at 15 psig. The carbon steel vessels were then hydrogen

PHOTO 0043-75
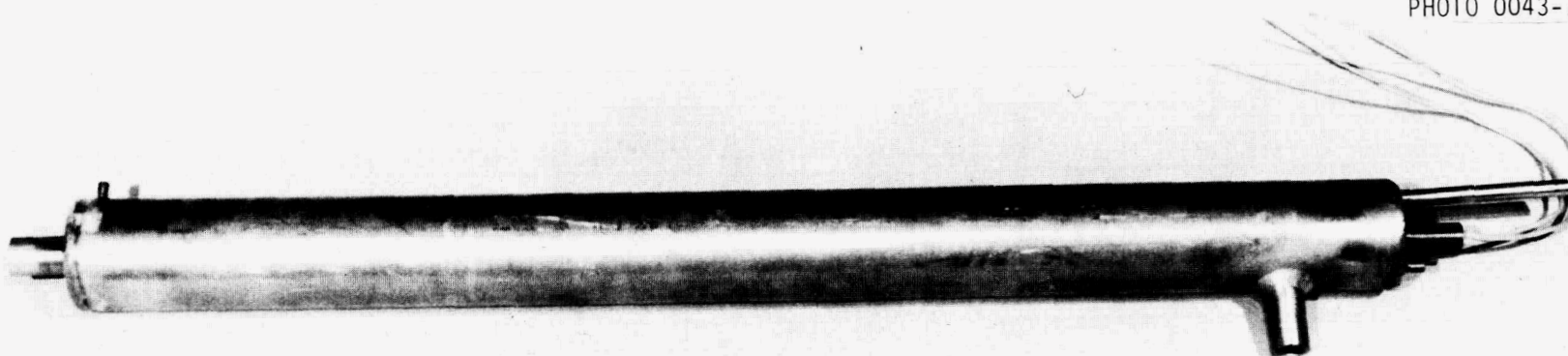
Fig. 7. Heat flowmeter used in autoresistance heating test AHT-4.

treated for ~ 7 hrs while at 650°C to remove oxides from the internal surfaces. Addition of the salt and bismuth phases to the process vessels was then begun. All additions were made from auxiliary charging tanks, and care was taken to prevent contamination of the materials before and during transfer into the process vessels. Finally, all salts and bismuth were filtered through a sintered molybdenum frit (~ 30-μ mean pore diameter) as they were transferred from the charging vessels into the process vessels to remove any particulates (such as oxides).

To date, we have completed the following additions to the MTE-3B process vessels:

(1) 61.7 kg of bismuth to the contactor vessel. The bismuth was hydrogen treated at 650°C to remove oxides.

(2) 110.6 kg of fuel carrier salt (72-16-12 mole % $LiF-BeF_2-ThF_4$) to the contactor and the fuel-salt reservoir. Before being added to the system, the fuel salt was sparged in the charging vessel with argon for 42 hr while in contact with bismuth which contained thorium.

The charging vessel used for the bismuth and fuel-carrier salt additions has been removed. A new charging vessel is being installed to facilitate the addition of a mixture of bismuth containing 5 at. % of lithium to the stripping vessel, and the lithium chloride addition to the contactor and stripper.

4. SALT-METAL CONTACTOR DEVELOPMENT: EXPERIMENTS WITH A MECHANICALLY AGITATED, NONDISPERSING CONTACTOR IN THE SALT-BISMUTH FLOWTHROUGH FACILITY

C. H. Brown, Jr.

We have continued operation of a facility in which mass transfer rates between molten $LiF-BeF_2-ThF_4$ (72-16-12 mole %) and molten bismuth can be measured in a mechanically agitated, nondispersing contactor of the "Lewis" type.[2] A total of nine experimental runs have been completed to date. Results from the first seven runs have been previously reported.[3,4] Preparation for and results obtained from the eighth and ninth runs, TSMC-8 and -9, respectively, are discussed in the following sections.

4.1 Preparation for Mass Transfer Experiments TSMC-8 and TSMC-9

In preparation for each of the runs made during this report period, it was necessary to: (1) add beryllium to the salt to adjust the uranium distribution coefficient; (2) contact the salt and bismuth by passing both phases through the mild steel contactor to ensure that chemical equilibrium was achieved between the salt and bismuth; and (3) add a sufficient quantity of ^{237}U tracer to the salt while it was in the salt feed tank. The experimental procedure that was followed in the first six runs has been previously reported,[3] and was followed in the last three runs.

4.2 Experimental Operation

Run TSMC-8 was performed with salt and bismuth flow rates of 152 cc/min and 164 cc/min, respectively. The uranium distribution coefficient was maintained at a high level (> 40) for this run, which, as has been previously discussed, is greater than the minimum desired value of 20. The agitator was thought to have been operated at 241 rpm, which is high enough to produce mild dispersion of the phases in the contactor and, therefore, results in a high measured mass transfer rate. Results from this run, however, indicated that very little (~ 25%) of the ^{237}U tracer was actually transferred from the salt to the bismuth. Inspection of the magnetically coupled agitator drive assembly indicated that an accumulation of a highly viscous, carbonaceous material between the upper carbon bearing and the agitator drive shaft had prevented proper rotation of the shaft. The drive assembly operated satisfactorily after it was cleaned of all foreign material and reassembled.

The ninth tracer run, TSMC-9, was performed as a repeat of the eighth run. Salt and bismuth flow rates were set at 169 cc/min and 164 cc/min, respectively. The agitator was operated at 244 rpm during this run. A high stirrer rate was maintained in order to determine the effects of dispersal of one phase in the other on the mass transfer rate, and to determine if large amounts of bismuth and salt are entrained in the other phase after passing through the small settling chamber in the contactor effluent line. The uranium distribution coefficient was greater than 47

during this run. No systematic problems were encountered and the run
was performed smoothly.

4.3 Mass Transfer Results

The samples taken during both runs were analyzed by first counting
the sample capsules for the activity of ^{237}U (207.95 keV β^-). The
material in the sample capsules was then dissolved, and the activity of
^{237}U was counted again. The counting data obtained in this manner for
runs TSMC-8 and TSMC-9 are shown in Tables 1 and 2, respectively.

Operating conditions and mass transfer results for runs TSMC-8 and
-9, and the results from runs TSMC-2 through -7 are summarized in Table 3.
The salt-phase mass transfer coefficient was calculated using three
different equations derived from an overall mass balance around the
contactor.[3] The average measured mass transfer coefficient, with the
corresponding standard deviation, is reported in Table 3.

As previously discussed, the agitator failed to operate properly in
run TSMC-8, which explains the rather low mass transfer rate measured
during this run, 0.0022 ± 0.0010 cm/sec. The measured mass transfer
coefficient obtained in run TSMC-9 is 0.121 ± 0.108 cm/sec, which
corresponds to 178% of the Lewis correlation. As shown by the high value
for the standard deviation, the three determinations for the mass transfer
coefficient differ greatly. One possible explanation for this is that
the ^{237}U tracer balance around the contactor showed closure to within
only 50%.

A Lewis plot of the results from the six runs which have produced
meaningful results is shown in Fig. 8. The nomenclature used in Fig. 8
is:

    k = individual phase mass transfer coefficient, cm/sec,

    ν = kinematic viscosity, cm^2/sec,

  Re = Reynolds Number (ND^2/ν), dimensionless,

    D = stirrer diameter, cm,

    N = stirrer rate, 1/sec,

  subscripts 1, 2 = phase being considered.

Table 1. Counting data obtained from run TSMC-8

Sample code[a]	Solid analysis for ^{237}U (counts/g)	Solution analysis for ^{237}U (counts/g)	Sample code[a]	Solid analysis for ^{237}U (counts/g)	Solution analysis for ^{237}U (counts/g)
			Samples taken prior to run		
358-B-5	$\leq 1.7 \times 10^3$	4.18×10^3	356-S-5	$\leq 3.8 \times 10^3$	
359-B-5	$\leq 1.4 \times 10^3$	4.33×10^3	357-S-5	$\leq 4.8 \times 10^3$	$\leq 8.9 \times 10^3$
362-B-1	1.27×10^3	4.51×10^3	360-S-3	$\leq 4.7 \times 10^3$	$\leq 1.6 \times 10^4$
363-B-1	1.25×10^3	4.06×10^3	301-S-3	$\leq 4.8 \times 10^3$	$\leq 1.6 \times 10^4$
			Samples taken prior to run but after addition of tracer		
			364-S-3	2.35×10^6	2.89×10^6
			365-S-3	2.41×10^6	2.91×10^6
			Samples taken during run		
366-B-FS	2.74×10^3	1.00×10^4	373-S-FS	3.04×10^5	3.73×10^5
367-B-FS	9.18×10^3	3.21×10^4	374-S-FS	9.45×10^5	1.02×10^6
368-B-FS	2.66×10^4	8.88×10^4	375-S-FS	1.76×10^6	2.14×10^6
369-B-FS	2.43×10^4	8.03×10^4	376-S-FS	2.08×10^6	2.29×10^6
370-B-FS	2.36×10^4	8.69×10^4	377-S-FS	1.94×10^6	1.90×10^6
371-B-FS	2.99×10^4	9.59×10^4	378-S-FS	1.90×10^6	2.18×10^6
372-B-FS	3.06×10^4	1.06×10^5	379-S-FS	2.43×10^6	2.34×10^6
			Samples taken after run		
380-B-1	4.78×10^3	1.57×10^4	384-S-3	2.28×10^6	2.67×10^6
381-B-1	4.81×10^3	1.48×10^4	385-S-3	2.10×10^6	2.48×10^6
382-B-2	1.51×10^4	5.22×10^4	386-S-4	1.77×10^6	2.15×10^6
383-B-2	1.56×10^4	4.07×10^4	387-S-4	1.80×10^6	2.35×10^6
388-B-5	1.22×10^5	3.19×10^5	390-S-5	$\leq 1.0 \times 10^4$	$\leq 2.4 \times 10^4$
389-B-5	1.39×10^5	3.66×10^5	391-S-5	$\leq 1.2 \times 10^4$	$\leq 2.4 \times 10^4$

[a]Each sample is designated by a code corresponding to A-B-C, where A = sample number; B = material in sample (B = bismuth, S = salt); and C = sample origin: 1 = T1, 2 = T2, 3 = T3, 4 = T4, 5 = T5, FS = flowing stream sample.

Table 2. Counting data obtained from run TSMC-9

Sample code[a]	Solid analysis for ^{237}U (counts/g)	Solution analysis for ^{237}U (counts/g)	Sample code[a]	Solid analysis for ^{237}U (counts/g)	Solution analysis for ^{237}U (counts/g)
		Samples taken prior to run			
394-B-5	$\leq 7.8 \times 10^2$	$\leq 3.2 \times 10^3$	392-S-5	$\leq 6.8 \times 10^3$	$\leq 1.3 \times 10^4$
395-B-5	$\leq 8.2 \times 10^2$	$\leq 2.6 \times 10^3$	393-S-5	$\leq 6.8 \times 10^3$	$\leq 1.3 \times 10^4$
398-B-1	7.64×10^2	$\leq 2.5 \times 10^3$	396-S-3	$\leq 6.7 \times 10^3$	$\leq 1.3 \times 10^4$
399-B-1	8.53×10^2	$\leq 3.0 \times 10^3$	397-S-3	$\leq 6.9 \times 10^3$	$\leq 1.2 \times 10^4$
		Samples taken prior to run but after addition of tracer			
			400-S-3	2.17×10^6	2.89×10^6
			401-S-3	2.18×10^6	3.25×10^6
		Samples taken during run			
402-B-FS	3.05×10^5	5.20×10^5	409-S-FS	2.17×10^5	1.94×10^5
403-B-FS	3.15×10^5	4.74×10^5	410-S-FS	2.06×10^5	2.16×10^5
404-B-FS	2.96×10^5	6.35×10^5	411-S-FS	2.04×10^5	2.00×10^5
405-B-FS	2.78×10^5	5.29×10^5	412-S-FS	1.96×10^5	1.95×10^5
406-B-FS	3.31×10^5	4.36×10^5	413-S-FS	2.22×10^5	1.79×10^5
407-B-FS	2.88×10^5	5.71×10^5	414-S-FS	1.74×10^5	1.88×10^5
408-B-FS	2.92×10^5	5.94×10^5	415-S-FS	1.89×10^5	1.69×10^5
		Samples taken after run			
416-B-1	8.55×10^2	$\leq 3.7 \times 10^3$	420-S-3	6.89×10^5	8.72×10^5
417-B-1	9.25×10^2	$\leq 3.1 \times 10^3$	421-S-3	7.12×10^5	8.65×10^5
418-B-1	1.47×10^5	3.05×10^5	422-S-4	1.54×10^5	1.81×10^5
419-B-2	1.43×10^5	2.86×10^5	423-S-4	1.54×10^5	1.69×10^5
424-B-5	1.08×10^5	2.29×10^5	426-S-5	$\leq 7.1 \times 10^3$	$\leq 1.5 \times 10^4$
425-B-5	1.19×10^5	2.45×10^5	427-S-5	$\leq 6.4 \times 10^3$	$\leq 1.4 \times 10^4$

[a]Each sample is designated by a code corresponding to A-B-C, where A = sample number; B = material in sample (B = bismuth, S = salt); and C = sample origin: 1 = T1, 2 = T2, 3 = T3, 4 = T4, 5 = T5, FS = flowing stream sample.

Table 3. Experimental results of mass transfer measurements in the salt-bismuth contactor

Run	Salt flow (cc/min)	Bismuth flow (cc/min)	Stirrer rate (rpm)	D_U	D_{Zr}	Fraction tracer transferred[a]	K_s (cm/sec) Based on U	K_s (cm/sec) Based on Zr
TSMC-2	228	197	121	0.94–34	0.96	0.17	0.0059 – 0.0092	0.0083 ± 0.0055
TSMC-3	166	173	162	> 34	--	0.50	0.012 ± 0.003	---
TSMC-4	170	144	205	> 172	> 24	0.78	0.054 ± 0.02	0.035 ± 0.02
TSMC-5	219	175	124	> 43	> 24	0.35	0.0095 ± 0.0013	0.0163 ± 0.0159
TSMC-6	206	185	180	> 172	> 24	0.64	0.039 ± 0.005	0.020 ± 0.01
TSMC-7	152	170	68	> 97	--	0.40	0.0057 ± 0.0012	---
TSMC-8	152	164	∿ 0	> 40	--	0.25	0.0022 ± 0.0010	---
TSMC-9	169	164	244	> 47	--	0.94	0.121 ± 0.108	---

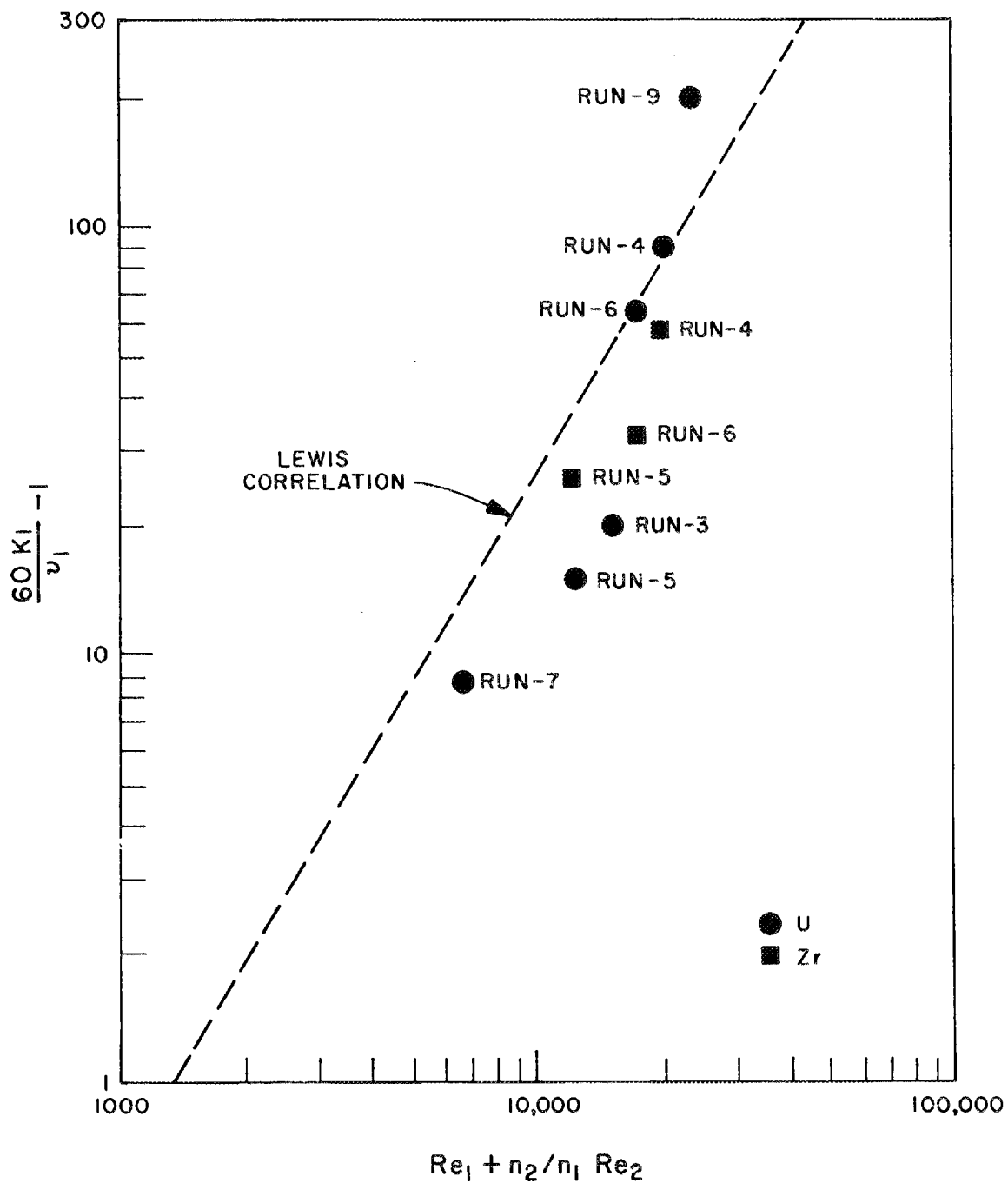[a]Fraction tracer transferred = $(1 - C_s/C_1)$.

17

ORNL DWG 75-758

Fig. 8. Mass transfer results measured in the salt-bismuth contactor with ^{237}U and ^{97}Zr tracers, compared to the values predicted by the Lewis correlation.

In Fig. 8 it can be seen that the mass transfer group based on uranium for runs 3, 5, and 7 is between 33% and 65% of the Lewis correlation, while that same group for runs 4, 6, and 9 is greater than 100% of the Lewis correlation. Run 8 was not shown because of the malfunction of the agitator drive. In all but one case, the mass transfer results based on zirconium are consistently slightly less than the values based on uranium. This discrepancy is probably related to the inability to correct for the self-absorption of the 743.37 keV β^- from the ^{97}Zr in the solid bismuth samples.

Results from the runs performed in the nondispersed regime, runs TSMC-3, -5, and -7, suggest that the dependence of the mass transfer group on the Reynolds number group is slightly less than that predicted by the Lewis correlation. The exponent appears to be closer to 1.0 than to 1.65. This is consistent with the Lewis data which show that for a single aqueous-organic system, the exponent on the Reynolds number group is more nearly 1.0 than 1.65.

We believe that the initiation of entrainment of salt into the bismuth begins to occur at a stirrer speed between 160 and 180 rpm. The apparent increase in mass transfer coefficient is a manifestation of an increase in the surface area for mass transfer due to surface motion. This effect is verified by the high mass transfer rates measured in runs 4, 6, and 9. Experiments with water-mercury and water-methylene bromide systems support the belief that phase dispersal is present at agitator speeds near 180 rpm.

It is possible that at high agitator rates (> 170 rpm) some salt or bismuth is entrained in the other phase and is carried out of the contactor. This effect is detectable if sufficient settling time is not available between the times when the salt and bismuth exit from the contactor and when the flowing stream samples are taken. Figure 9 shows the results of analysis for beryllium in the bismuth flowing stream samples taken in runs TSMC-5, -6, and -9, which were performed at 124, 180, and 244 rpm, respectively.
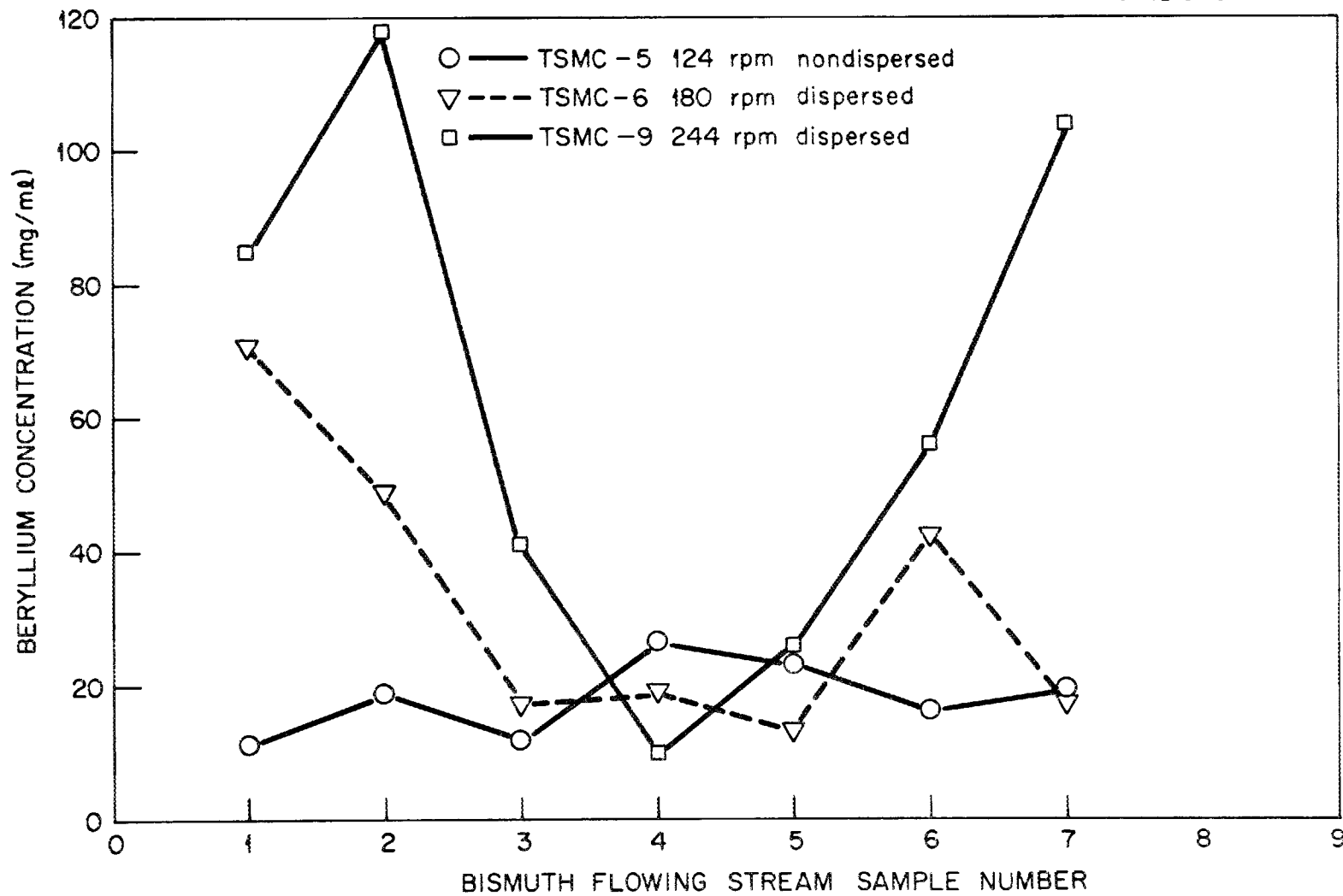
Fig. 9. Beryllium concentration in the bismuth flowing stream samples.

It is assumed that any beryllium present in the salt is due to entrainment of salt in the bismuth phase. From Fig. 9, it is seen that when dispersion is suspected there is more beryllium, and hence salt, present in the bismuth stream, at least near the beginning and near the end of a run. In the middle of a run, agitator speed does not seem to have an effect on the amount of beryllium in the bismuth. The effect of salt entrainment in the bismuth is most significant in the metal transfer process where the presence of fluoride ions in the lithium chloride has a deleterious effect on the separation between the rare earths and thorium.

Analyses of bismuth in the salt samples could not be obtained. However, no gross amounts of bismuth were indicated from the weights of the salt samples. It is possible to take advantage of the increased mass transfer rate afforded by mild dispersal of the salt and bismuth phases in a stirred contactor without imposing any detrimental effects to the reactor vessel, or adding a large burden to the bismuth removal step. We plan to make a series of runs at high agitator speeds to investigate more closely the magnitude of entrainment effects in this type of contactor.

5. SALT-METAL CONTACTOR DEVELOPMENT: EXPERIMENTS WITH A MECHANICALLY AGITATED, NONDISPERSING CONTACTOR USING WATER AND MERCURY

C. H. Brown, Jr.

We have continued development of a two-phase nondispersing contactor using water and mercury to simulate molten fluoride salt and bismuth.

During this report period, several runs were made in the water-mercury system at an elevated temperature to determine if the assumption that the reaction under consideration,

$$Pb^{2+}\left[H_2O\right] + Zn\left[Hg\right] \rightarrow Zn^{2+}\left[H_2O\right] + Pb\left[Hg\right], \tag{1}$$
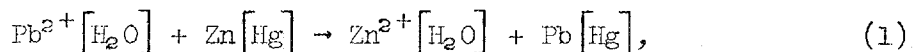
is instantaneous. We have also initiated experiments to determine if polarography is a viable alternative method for determining individual

water-phase mass transfer coefficients in the nondispersing stirred interface contactor.

5.1 Runs at Elevated Temperatures with the Lead Ion-Zinc Amalgam System

Several runs were made in which the temperature of the contactor and reactants was raised to approximately 40°C. The results from these tests are inconclusive, because it was found that at this elevated temperature, hydrochloric acid, which was present in the aqueous phase to prevent oxide formation at the mercury surface, reacted with zinc to form zinc chloride. This makes the mass transfer analysis more difficult by introducing a competing reaction. Also, depletion of the acid caused formation of a spongy lead compound on the agitator blades and at the water-mercury interface.

5.2 Polarographic Determination of Mass Transfer Coefficients

Polarography has been suggested as an alternate method for determining the water-phase mass transfer coefficient in the water-mercury contactor. The necessary experimental equipment has been assembled and preliminary tests have been made to determine: (1) a suitable redox couple, and (2) an electrolyte which will produce the desired polarization curve while being chemically inert to mercury.

5.2.1 Theory

The polarographic technique for determining mass transfer coefficients involved oxidation of a reduced species or reduction of an oxidized species at an electrode which is at a condition of concentration polarization.

One system that has been studied previously[5] is the reduction of ferricyanide ions at a polarized nickel electrode. As ferricyanide was reduced at the cathode, ferrocyanide was oxidized at the anode. There was no net consumption of chemicals or change in the composition of the electrolyte solution.

Polarization of the cathode can be accomplished in one of two ways -- either the cathode surface area is made very large with respect to the

anode surface area, or the concentration of the oxidized species is made
very small with respect to the reduced species.

The migration of an ion in both electric and concentration fields
is described by the Nernst-Planck equation:

$$Q = D(\nabla C + \frac{ZCF}{RT} \nabla \Phi), \qquad (2)$$

where

C = concentration of reacting ion, moles/liter,

Q = flux of the ion, moles $cm^{-2} sec^{-1}$

D = diffusion coefficient, cm^2/sec,

Z = valence change of the transferring ion,

R = gas constant,

T = absolute temperature, °K,

F = Faraday constant, °C/mole,

Φ = electric potential, V.

The first term in the expression represents the contribution of ordinary
diffusion to the flux, and the second term represents the contribution of
electromigration. A large concentration (relative to that of the reacting
ion) of an inert electrolyte alters the dielectric properties of the
solution such that the potential will decrease smoothly across the region
between the electrodes, while the concentration drops sharply across the
thin polarized layer near the cathode. Thus, the term containing the
electric potential becomes relatively small, and

$$Q \approx D\nabla C. \qquad (3)$$

The current flowing between the electrodes is thus a measure of mass
transfer rates governed by ordinary molecular diffusion. This current
is sometimes called the "diffusion current."

The impressed current across the cell is proportional to the mass
flux across the stagnant layer between the bulk electrolyte and the
polarized cathode, and the mass transfer coefficient is given by:

$$K = \frac{I}{(Z)\ (A)\ (F)\ (C_B)}, \tag{4}$$

where

k = mass transfer coefficient through the film, cm/sec,

I = polarization current, A,

A = area of the polarized electrode, cm^2, and

C_B = concentration in g-moles/cm^3 of transferring species in the
bulk liquid.

Hence, it is possible to determine mass transfer rates from the bulk
electrolyte to the electrode surface using experimentally determined values
for I, C_B, and A.

5.2.2 Experimental equipment

The experimental apparatus which will be used to measure mass trans-
fer rates in the water-mercury stirred contactor is shown schematically
in Fig. 10. The equipment consists of the 5- by 7-in. Plexiglas contactor
which was used in previous work with the water-mercury system. The
mercury surface in the contactor acts as the cathode in the electrochemical
cell. The cathode is electrically connected to the rest of the circuit
by a 1/8-in.-diam stainless steel welding rod which is electrically
insulated from the electrolyte phase by a Teflon sheath. The anode of
the cell is suspended in the aqueous electrolyte phase, and consists of
a 1/8-in.-thick piece of nickel sheet which is formed to fit the inner
perimeter of the Plexiglas cell. The current through the cell is inferred
from the voltage drop across a 0.1 Ω ± 0.5%, 10-W precision resistor. The
signal produced across the resistor is recorded as the y coordinate on a
Hewlett-Packard x,y plotter. The x coordinate on the plotter is produced
by the voltage supplied to the cell, which is a direct signal from the
0 to 10 V, 0 to 10 A Hewlett-Packard direct current power supply.

5.2.3 Experimental results

Several different electrolyte solutions have been evaluated on the
basis to two different criteria: (1) the electrolyte must be chemically
inert to mercury, and (2) it must be possible to polarize the mercury sur-
face with the given electrolyte. The different electrolytes that have

X,Y PLOTTER

VARIABLE SPEED
DRIVE MOTOR

"x"   "y"
+   -   +   -

R
0.1 Ω
10 WATTS

H₂O

Hg

D C POWER SUPPLY
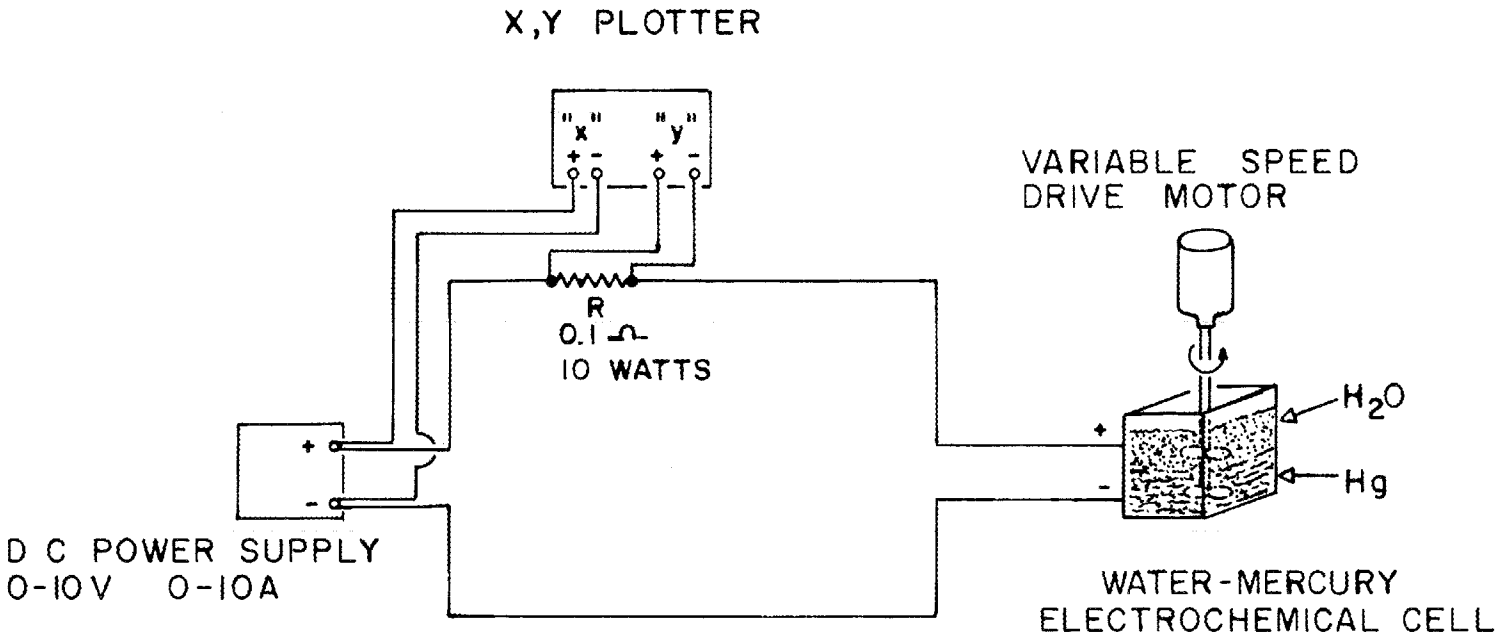0-10 V   0-10 A

WATER-MERCURY
ELECTROCHEMICAL CELL

Fig. 10. Schematic diagram of the equipment used to measure polari-
zation currents in the water-mercury electrochemical cell contactor.

been examined are: (1) potassium ferro- and ferricyanide with a sodium hydroxide supporting electrolyte; (2) potassium ferro- and ferricyanide with a sodium chloride supporting electrolyte; (3) potassium ferro- and ferricyanides with a sodium nitrate supporting electrolyte; (4) ferrous and ferric sulfate with a sodium hydroxide supporting electrolyte; and (5) ferrous and ferric sulfate with sulfuric acid as the supporting electrolyte.

None of the electrolytes mentioned above met both of the imposed criteria. The ferrous and ferric sulfate system with sulfuric acid as the indifferent electrolyte was the only combination which proved to be chemically inert to the mercury cathode. It was found, however, that at a voltage less than sufficient to polarize the mercury cathode, the ferric ions reacted with the mercury cathode. This phenomenon has been previously reported in the literature.[6]

Kolthoff and Lingane[6] report that the following reaction occurs when ferric ions are contacted with mercury:

$$2 \ Fe^{3+} \ 2 \ Hg = 2 \ Fe^{2+} + Hg_2^{2+} \ ; \tag{5}$$
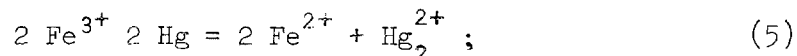
therefore, the half-wave potential of ferric ions cannot be measured directly.

The reversible oxidation and reduction of ferrous and ferric ions have been reported feasible when the iron ions are complexed with excess oxalate ions. This system will be examined in detail and applied to the experiment under development.

6. FUEL RECONSTITUTION DEVELOPMENT: INSTALLATION OF EQUIPMENT FOR A FUEL RECONSTITUTION ENGINEERING EXPERIMENT

R. M. Counce

The reference flowsheet for processing the fuel salt from a molten salt breeder reactor (MSBR) is based upon removal of uranium by fluorination to UF_6 as the first processing step. The uranium removed in this step must subsequently be returned to the fuel salt stream before it

returns to the reactor. The method used for recombining the uranium with the fuel carrier salt (reconstituting the fuel salt) is to absorb gaseous UF_6 into a recycled fuel salt stream containing dissolved UF_4 by utilizing the reaction:

$$UF_{6(g)} + UF_{4(d)} = 2 UF_{5(d)} \quad .\tag{6}$$
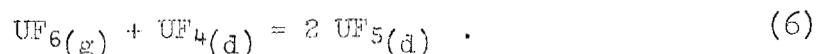
The resultant UF_5 would be reduced to UF_4 with hydrogen in a separate vessel according to the reaction:

$$UF_{5(d)} + 1/2 H_{2(g)} = UF_{4(d)} + HF_{(g)} .\tag{7}$$
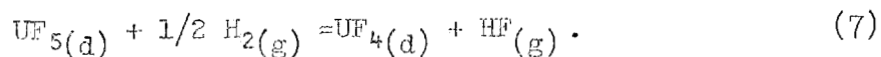
We are beginning engineering studies of the fuel reconstitution step in order to provide the technology necessary for the design of larger equipment for recombining UF_6 generated in fluorinators in the processing plant with the process fuel salt returning to the reactor. During this report period, installation of equipment previously described[7] was continued. This report describes the general gas supply systems, documents the equipment installation, and describes the initial salt preparation.

6.1 Gas Supply Systems

The UF_6 for the fuel reconstitution engineering experiment is available in 5-in.-diam by 36-in.-high cylinders containing up to 55 lb of UF_6. The $UF_{6(g)}$ will be supplied to this experiment by maintaining the temperature of the UF_6 cylinder at 220°F, and at a vapor pressure of 70 psia. This heating will be accomplished by use of 17.2-psia steam.

The steam heats the cylinders directly through 3/8-in. copper tubing, which is coiled around the entire cylinder. The lower 18 in. of the cylinder and tubing is covered with a conductive cement to minimize response time. The cylinder and associated valves are then enclosed in a cabinet insulated with 2 in. of Fiberglas insulation.

Purified argon will be used for all applications requiring an inert gas (e.g., pressurization of tanks for transferring salt, dip-leg bubblers for liquid level measurements, purging of equipment and lines, etc.). Cylinder argon is passed through a bed of titanium sponge where water and oxygen are removed. This bed operates at 825°C.

Cylinder hydrogen is purified sufficiently by passing it through a Deoxo unit, where oxygen is converted to water. No further purification of the nitrogen is needed, since it is sufficiently pure for use in calibrating the gas density cells.

6.2 Equipment Installation

The equipment for the fuel reconstitution engineering experiment is being installed in the northeast corner of the bay in Building 7503. The experiment is operated remotely from a control room in the building, although the gas flow controllers and some other equipment are located in the bay.

The experimental equipment is shown in Figs. 11-14 before the addition of thermal insulation. Fig. 11 is an overall sideview of the equipment showing the feed and receiver tanks, titanium sponge trap, H_2 reduction column and its jackleg and sample port, and the HF and UF_6 traps. Figure 12 is an overall front view of the experiment showing the gas control panel feed and receiver tanks, the top of the UF_6 absorption vessel, and the H_2 reduction column and its effluent stream sample port. Figure 13 shows a view of the lower portion of the H_2 reduction column and its jackleg, and the instruments for measuring the depth of the feed and receiver tanks. A view of the HF and UF_6 traps (packed beds of NaF pellets) and the in-line gas density detectors is shown in Fig. 14.

The electrical supply panel is located in a remote control room, and is shown in Fig. 15. Temperature is controlled by manual adjustment of heater voltage and by automatic on-off controllers.

Figure 16 shows the temperature recorders and temperature controllers for major vessels and the gas density cells. Also shown are level and flow recorders and controllers. The instruments at the right of the control panel are recorders associated with the gas density cells.

ORNL-Photo 1153-75R1

EFFLUENT STREAM
SAMPLER

H₂ REDUCTION
COLUMN
JACKLEG

FEED
TANK

RECEIVER
TANK

H₂ REDUCTION
COLUMN

GAS SUPPLY
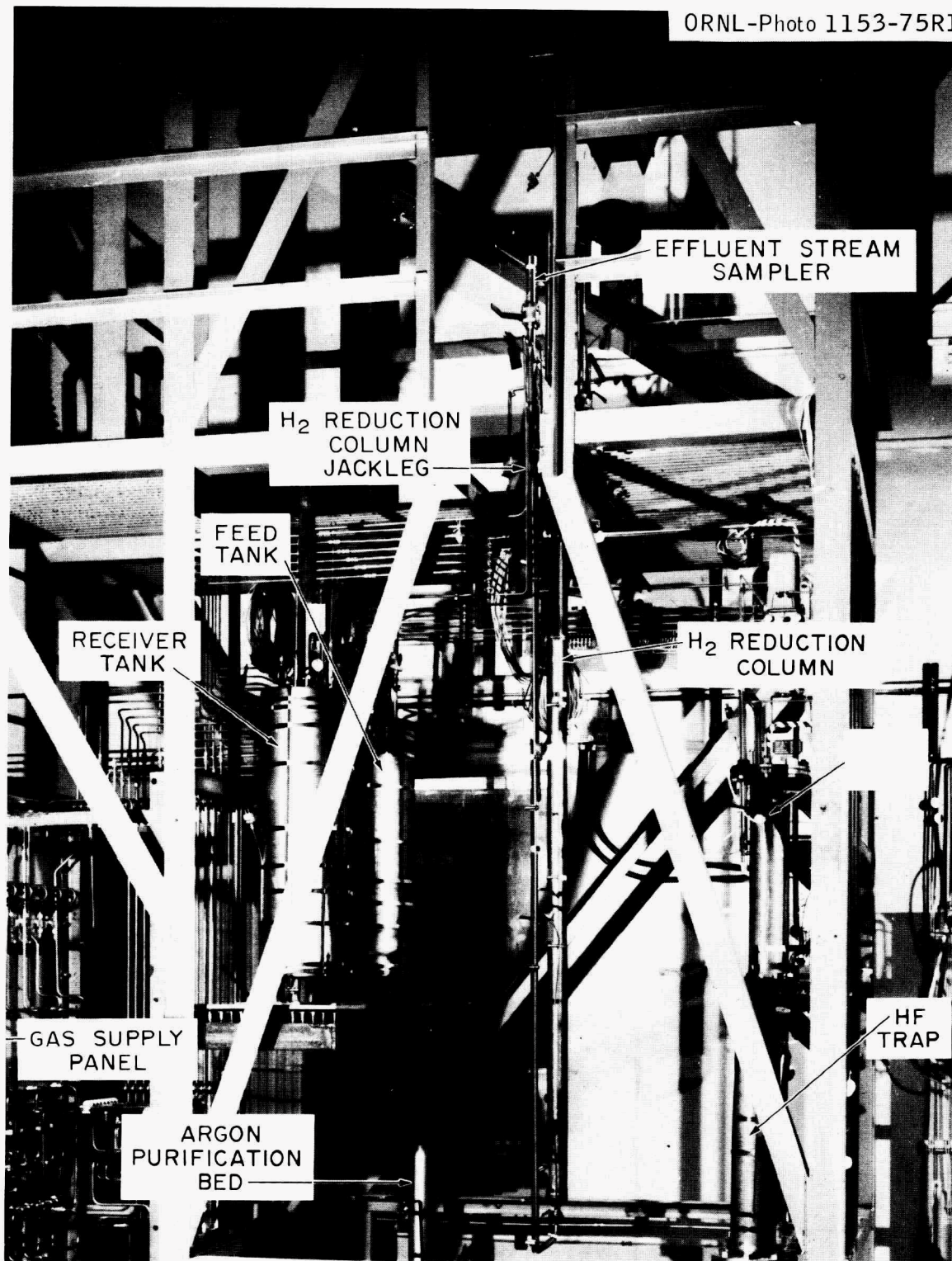PANEL

HF
TRAP

ARGON
PURIFICATION
BED

Fig. 11. Overall side view of equipment for Fuel Reconstitution
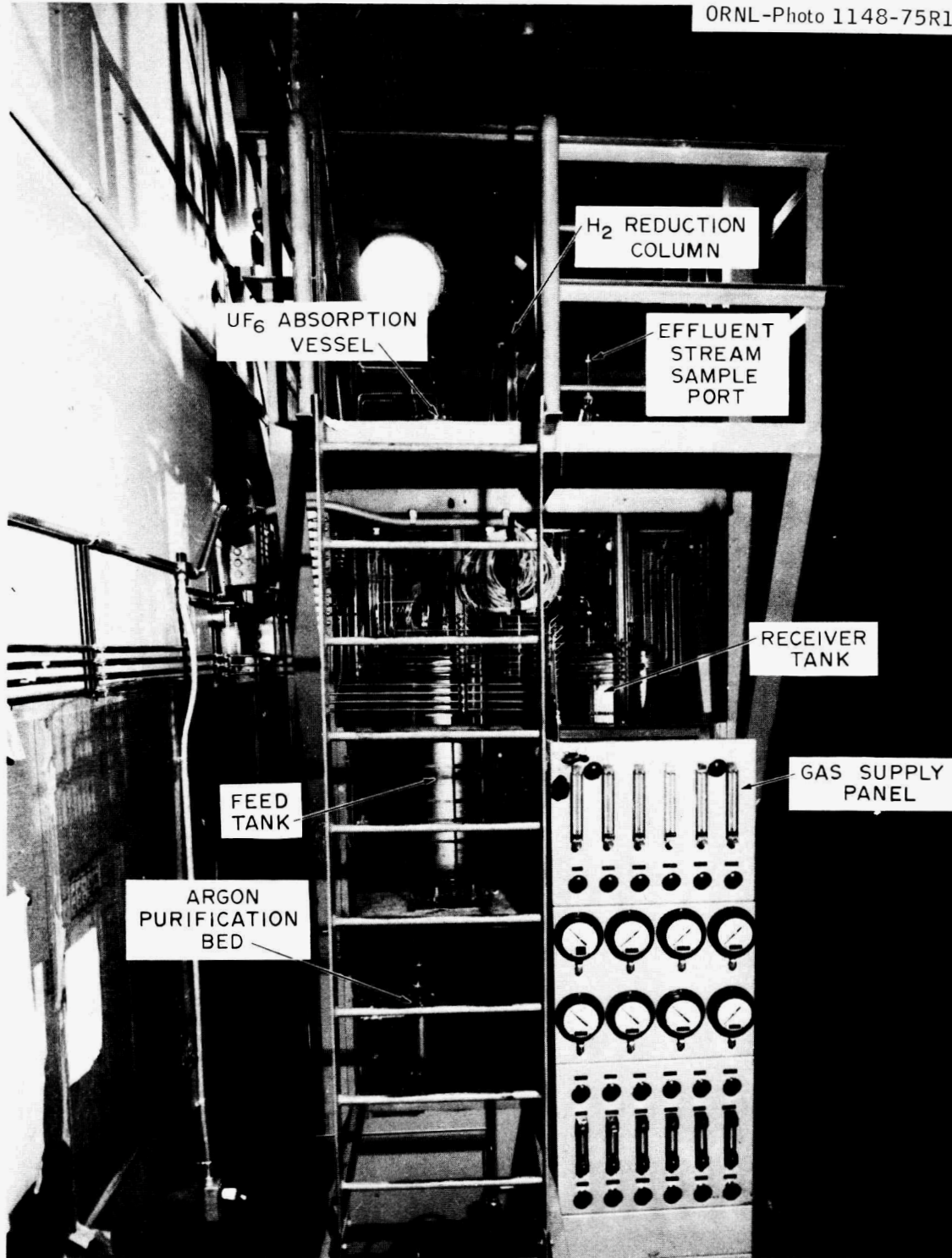Engineering Experiment before addition of thermal insulation.

Fig. 12. Overall front view of Fuel Reconstitution Engineering
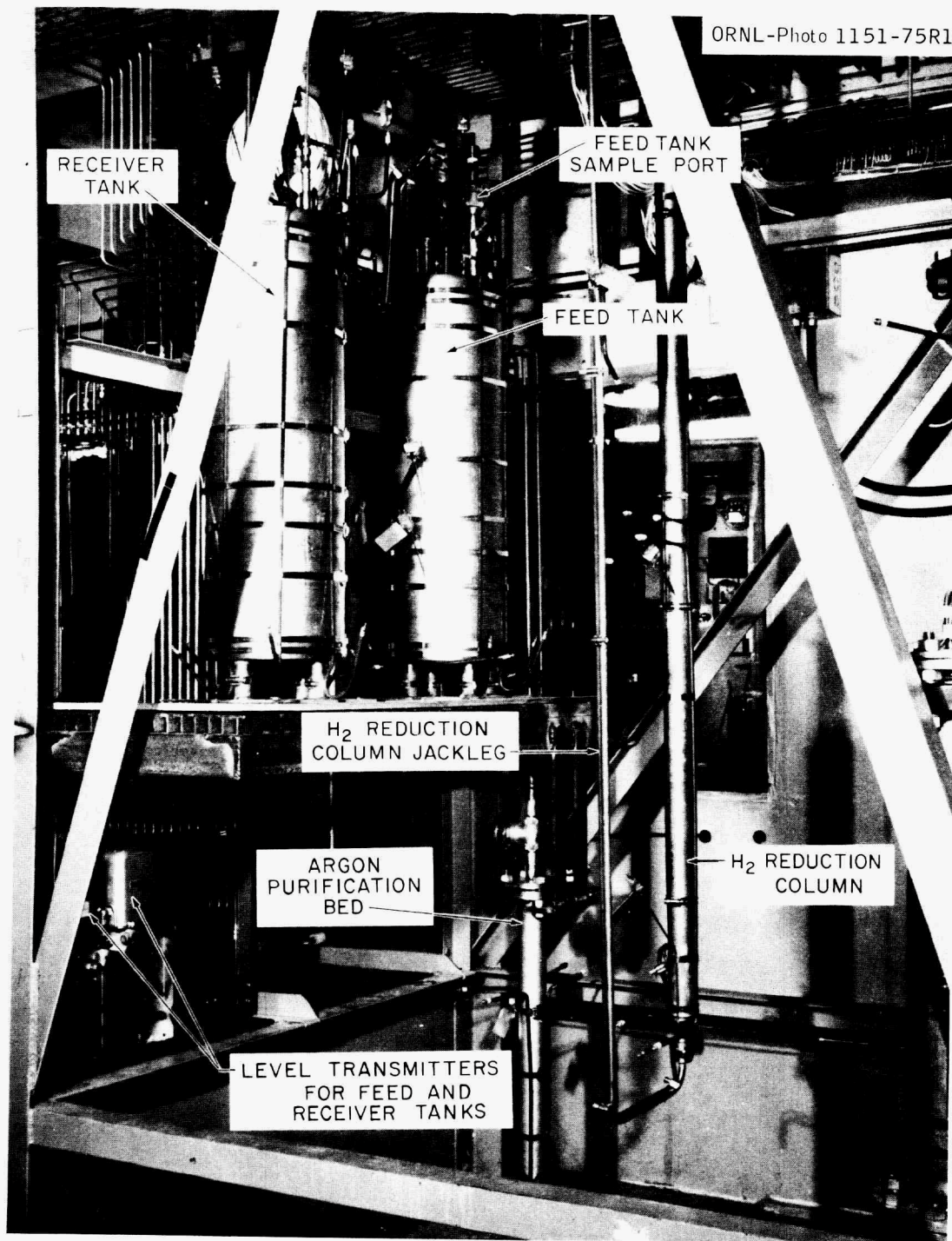Experiment showing gas control panel.

Fig. 13. View of installed feed tank and receiver, titanium sponge trap, and bottom of hydrogenation column.
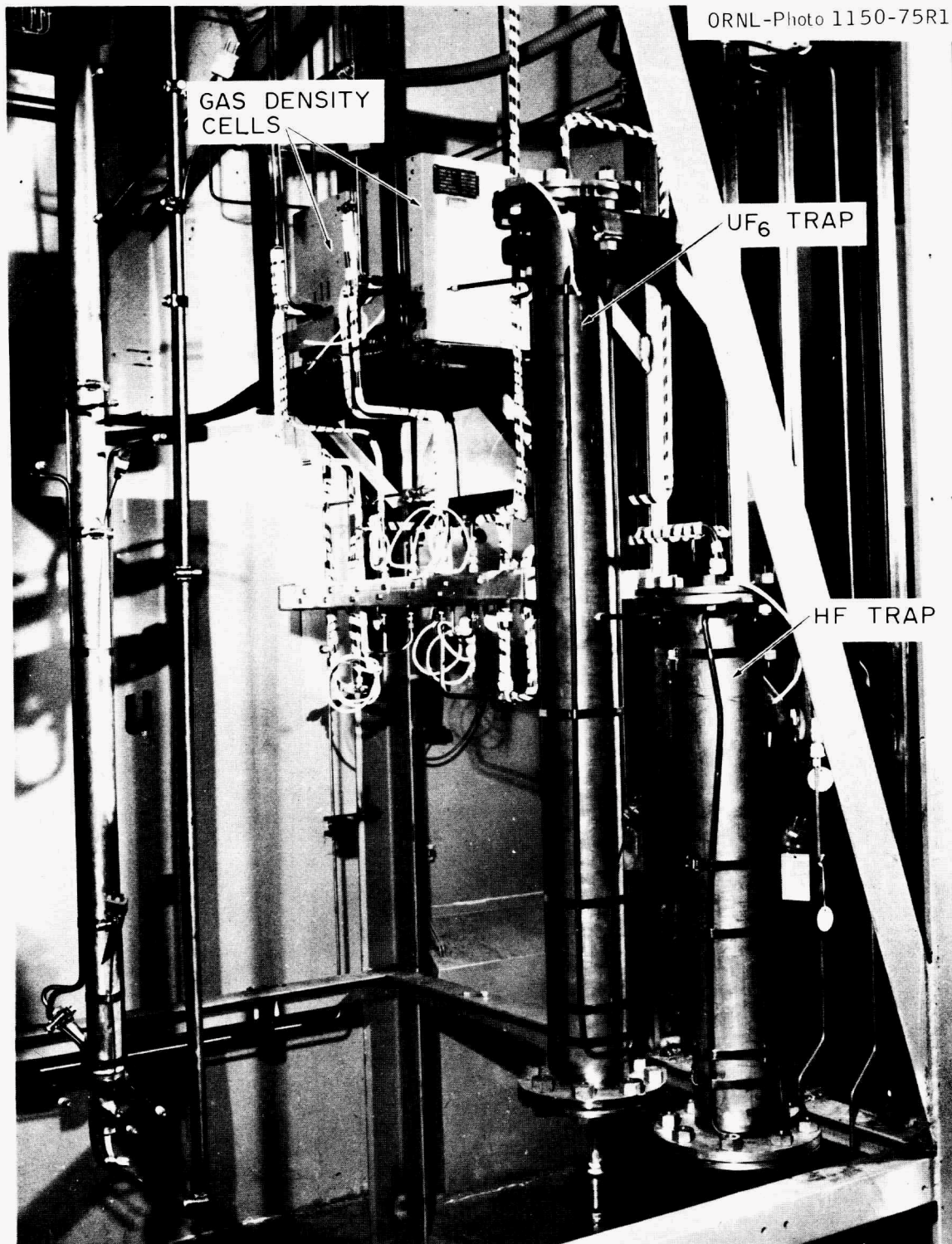
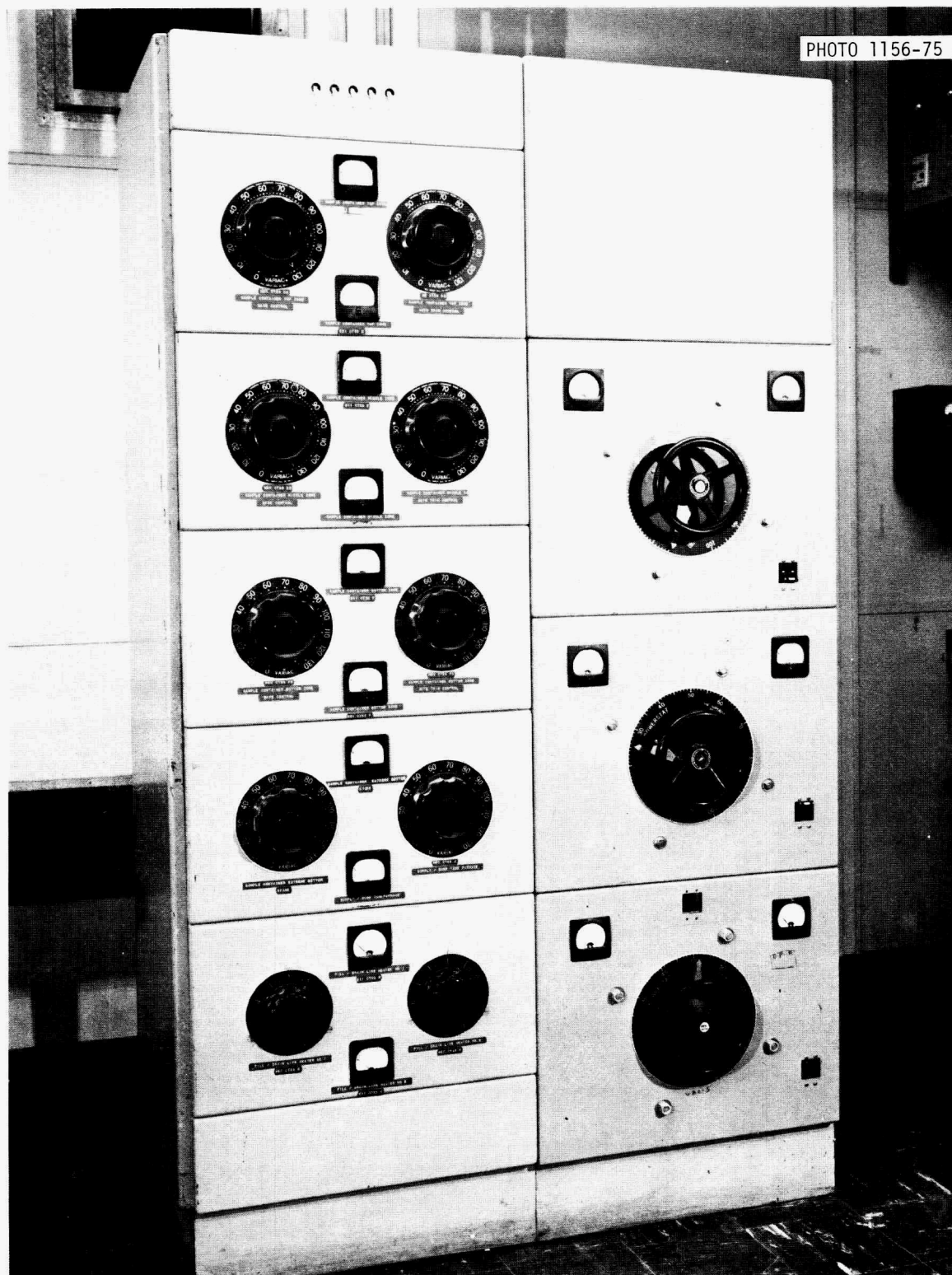Fig. 14. View of sodium fluoride traps and in-line gas density detectors.

Fig. 15. Electrical supply panel for Fuel Reconstitution Engineering
Experiment.

Fig. 16. Panelboard for Fuel Reconstitution Engineering Experiment temperature, level, and flow recorders and controllers.

6.3 H_2-HF Treatment of Salt from Autoresistance Heating Tests

The first series of experiments will use 86 kg of fuel salt, formerly used in AHT-3. To remove oxides present in the salt, it was sparged with a H_2-HF mixture in Bldg. 3541. The metal oxides were removed according to the following generalized reaction:

$$XHF(g) + MOx/2(d) \rightleftarrows MF_x(d) + x/2\ H_2O(g), \qquad (8)$$
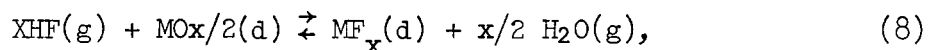
where

    (g) = gaseous

    (d) = dissolved

    x = number of moles

    M = metal species found in salt.

The HF was diluted with H_2 in order to prevent excessive attack on vessel and piping. The HF concentration in the mixture was 33 vol %. The nominal total flow rate was 15 scfh.[*] The HF flow was set by controlling the pressure drop across a capillary; the H_2 flow was set by use of a rotameter and was checked by a wet-test meter.

The HF utilization was determined by using an aqueous scrubber and a small (0.05 ft^3/rev) wet-test meter in parallel with the NaF trap for sampling the gas fed to the treatment vessel or leaving the vessel. The concentration of HF in the gas stream was determined by passing the gas through 250 ml of a 0.4 $\underline{N}$ NaOH solution in the scrubber. When 0.05 ft^3 of H_2 had passed through the wet-test meter, the gas flow was stopped and the solution was removed for analysis. The HF concentration in the gas was determined by titrating small samples of the scrubbing solution with 0.1 $\underline{N}$ HCl. Both the feed and the discharge streams were monitored in this manner. Utilization of the HF was calculated from the feed and discharge concentrations. The HF utilization decreased from an initial value of about 50% to about 25% after 20 hr. The HF utilization remained at 25% for the last 10 hr.

---

[*]Standard cubic feet per hour.

Reduction of corrosion product fluorides, principally NiF_2, FeF_2, and CrF_2, will proceed after verification of oxide removal. Of the corrosion products present in the salt, a hydrogen sparge will reduce only NiF_2 in a practical time period; thus, CrF_2 and possibly FeF_2 will be reduced with Th metal.

After the reduction of the corrosion fluorides to their metallic form, they will be filtered from the mixture as it is decanted into a fuel reconstitution experiment vessel. Sufficient UF_4 will be added to bring the concentration in the salt to 0.0125 mole % after the salt has been transferred to the fuel reconstitution equipment.

7. REFERENCES

1. H. C. Savage, *Engineering Development Studies for Molten-Salt Breeder Reactor Processing No. 20*, ORNL-TM-4870 (in preparation).

2. J. B. Lewis, Chem. Eng. Sci. 3, 248-59 (1954).

3. J. A. Klein, *MSR Program Semiann. Progr. Rept. Aug. 31, 1974*, ORNL-5011.

4. C. H. Brown, Jr., *MSR Program Semiann. Progr. Rept. Feb. 28, 1975*, ORNL-5047.

5. J. S. Watson, "A Study of Detached Turbulence Promoters for Increasing Mass Transfer Rates in Aqueous Chemical Flow," Ph.D. Thesis, University of Tennessee (1967).

6. I. M. Kolthoff and J. J. Lingane, *Polarography*, 1st ed., Interscience, New York, 1946.

7. R. M. Counce, *Engineering Development Studies for Molten-Salt Breeder Reactor Processing No. 20*, ORNL-TM-4870 (in preparation).

ORNL/TM-4894
UC-76 — Molten Salt Reactor Technology

INTERNAL DISTRIBUTION

1-2.	MSRP Director's Office	40.	W. R. Grimes
3.	C. F. Baes, Jr.	41.	R. H. Guymon
4.	C. E. Bamberger	42-51.	J. R. Hightower, Jr.
5.	J. Beams	52.	B. F. Hitch
6.	M. Bender	53.	R. W. Horton
7.	M. R. Bennett	54.	W. R. Huntley
8.	E. S. Bettis	55.	V. A. Jacobs
9.	R. E. Blanco	56.	C. W. Kee
10.	J. O. Blomeke	57.	A. D. Kelmers
11.	E. G. Bohlmann	58.	W. R. Laing
12.	J. Braunstein	59.	R. B. Lindauer
13.	M. A. Bredig	60.	R. E. MacPherson
14.	R. B. Briggs	61.	W. C. McClain
15.	H. R. Bronstein	62.	H. E. McCoy
16.	R. E. Brooksbank	63.	A. P. Malinauskas
17.	C. H. Brown, Jr.	64.	C. L. Matthews
18.	K. B. Brown	65.	R. L. Moore
19.	J. Brynestad	66.	J. P. Nichols
20.	S. Cantor	67.	H. Postma
21.	D. W. Cardwell	68.	M. W. Rosenthal
22.	W. L. Carter	69.	H. C. Savage
23.	W. H. Cook	70.	W. F. Schaffer, Jr.
24.	R. M. Counce	71.	C. D. Scott
25.	J. L. Crowley	72.	M. J. Skinner
26.	F. L. Culler	73.	F. J. Smith
27.	J. M. Dale	74.	G. P. Smith
28.	F. L. Daley	75.	I. Spiewak
29.	J. H. DeVan	76.	O. K. Tallent
30.	J. R. DiStefano	77.	L. M. Toth
31.	W. P. Eatherly	78.	D. B. Trauger
32.	R. L. Egli, AEC-OSR	79.	W. E. Unger
33.	J. R. Engel	80.	J. R. Weir
34.	G. G. Fee	81.	M. K. Wilkinson
35.	D. E. Ferguson	82.	R. G. Wymer
36.	L. M. Ferris	83-84.	Central Research Library
37.	L. O. Gilpatrick	85.	Document Reference Section
38.	W. S. Groenier	86-88.	Laboratory Records
39.	J. C. Griess	89.	Laboratory Records (LRD-RC)

CONSULTANTS AND SUBCONTRACTORS

90. J. C. Frye
91. C. H. Ice
92. J. J. Katz
93. E. A. Mason
94. Ken Davis
95. R. B. Richards

EXTERNAL DISTRIBUTION

96. Research and Technical Support Division, ERDA, Oak Ridge
Operations Office, P. O. Box E, Oak Ridge, Tenn. 37830
97. Director, Reactor Division, ERDA, Oak Ridge Operations
Office, P. O. Box E, Oak Ridge, Tenn. 37830
98-99. Director, ERDA Division of Reactor Research and Development,
Washington, D. C. 20545
100-201. For distribution as shown in TID-4500 under UC-76, Molten
Salt Reactor Technology